Check for updates

Journal of
Materials Chemistry C

Accepted Manuscript

This article can be cited before page numbers have been issued, to do this please use: M. Wasala, H. Sirikumara, Y. R. Sapkota, S. Hofer, D. Mazumdar, T. Jayasekera and S. Talapatra, *J. Mater. Chem. C*, 2017, DOI: 10.1039/C7TC02866K.

This is an Accepted Manuscript, which has been through the Royal Society of Chemistry peer review process and has been accepted for publication.

Accepted Manuscripts are published online shortly after acceptance, before technical editing, formatting and proof reading. Using this free service, authors can make their results available to the community, in citable form, before we publish the edited article. We will replace this Accepted Manuscript with the edited and formatted Advance Article as soon as it is available.

You can find more information about Accepted Manuscripts in the author guidelines.

Please note that technical editing may introduce minor changes to the text and/or graphics, which may alter content. The journal's standard Terms & Conditions and the ethical guidelines, outlined in our author and reviewer resource centre, still apply. In no event shall the Royal Society of Chemistry be held responsible for any errors or omissions in this Accepted Manuscript or any consequences arising from the use of any information it contains.

ROYAL SOCIETY OF CHEMISTRY

rsc.li/materials-c

View Article Online
DOI: 10.1039/C7TC02866K

Published on 20 October 2017. Downloaded by Gazi Universitesi on 21/10/2017 19:45:29.

Journal of Materials Chemistry C Accepted Manuscript

Recent Advances in Investigations of Electronic and Optoelectronic Properties of Group III, IV, and V Selenide Based Binary Layered Compounds

Milinda Wasala, Hansika I. Sirikumara, Yub Raj Sapkota, Stephen Hofer, Dipanjan Mazumdar, Thushari Jayasekera and Saikat Talapatra*

This review article presents a comprehensive update on recent research trends, advancement and future outlook of selected layered selenide-based binary compounds featuring elements from group III, IV, and V of the periodic table. Due to their highly anisotropic structure as well as their availability in mono, few and multi-layer form, these compounds constitute a perfect playground where a variety of possibility in structural variation as well as functionalities are expected. This potentially gives rise to a library of unique and fascinating 2D selenide-based systems. These systems appear to demonstrate some spectacular variety of fundamental physics as well as indicate that some of these systems can be beneficial for several niche applications directly or indirectly resulting from their electrical and optical properties. As such a description of recent investigations pertaining to some of the key electrical and optical properties of few chosen binary selenide based compounds such as Indium Selenide, Tin Selenide, Gallium Selenide, Germanium Selenide and Bismuth Selenide are described. A final note on immediate research needs and directions in developing these materials systems for future applications are discussed.

1 Introduction

The breathtaking success of graphene science, discovery of families of layered Van der Waals solids, their hetero-structures and hybrids, and realization of rich and exotic band structure of various other two dimensional (2D) layered materials, have opened up several new directions in the understanding of science and technology of 2D layered systems. During the last decade, 2D layered materials have caused a paradigm shift in our understanding of the fundamental properties of nanomaterials and opened up new technological possibilities. The discovery of single-layer graphene[1–3] and transition metal dichalcogenides (TMDs)[4,5], initially through mechanical exfoliation have sparked a series of high profile discoveries that impact numerous electronic and optoelectronic areas[6–8]. Several of these materials were also viewed as potential candidates for future applications as well[9].

The tremendous scientific accomplishments, primarily in the field of graphene science and later in identifying TMD based 2D materials also led to the discovery of or at least gave the impetus to search for a wide variety of compounds, with 2D layered structure, which can possibly be reduced to few atomic layers. One of the key reasons, other than the fact that materials with 2D atomic configurations are extremely interesting from fundamental science[1–3], their flat topography is perhaps ideally suited for compatibility with present complementary metal oxide semiconductor (CMOS) technology that drives the electronic industry. As such a major portion of investigations on 2D materials in general focused on their electronics/opto-electronics aspect[4–6,9,10]. Several key fundamental physical properties were also recognized. For example, unlike graphene, which is a zero band semimetal, a single layer of some TMDs such as Molybdenum disulphide (MoS_2) has a direct band gap[11] and can be used as a field effect transistor. This was an extremely important finding, which initiated investigations pertaining to optics/optoelectronic properties of 2D materials other than graphene. In that aspect, as described in this article later, some of the layered selenides that we are planning to present here, have a major advantage over other TMD based layered materials.

2 Unique Properties of Layered Selenide Based Materials

One of the main motivation behind investigating layered selenides stems from the fact that these systems can exhibit diverse structural form in the bulk, which leads to multi-functional properties such as thermoelectric[12–14], optoelectronics[15–17] etc. Out of all selenides, elements of group III, IV and V forms selenide based layered structures, which is mediated through a lone electron pair. The lone electron pair repels the neighboring atoms, thus creating a van der Waals gap between chemically bound layers[18]. The fact that many of these, for example, InSe (III-

Department of Physics, Southern Illinois University Carbondale, Illinois - 62901. Fax: 618 453 1056; Tel: 618 453 2270; E-mail: stalapatra@physics.siu.edu

View Article Online
DOI: 10.1039/C7TC02866K
Published on 20 October 2017. Downloaded by Gazi Universitesi on 21/10/2017 19:45:29.
Journal of Materials Chemistry C Accepted Manuscript

VI), SnSe (IV-VI), BiSe (V-VI) and their polytypes possess saturated bonds (with no dangling electrons) make them ideal as two-dimensional electron systems [18]. Few/mono layers of these specific selenides, similar to those other 2D materials, show very different but diverse attractive properties compared to their bulk form. For example, selenides in the III-VI (eg: InSe) and IV-VI (eg: SnSe) are very good optoelectronic materials, but lately SnSe have also shown to possess other functional properties such as high thermoelectric figure-of-merit (ZT) [12]. Bi_2Se_3 is another fascinating layered system. While it is known to be a great thermoelectric material, recently it is being investigated as a topological insulator. Layered InSe is predicted to undergo semiconducting to metal transition under electric field application, making it ideal for memory applications [19]. Similarly, theoretical calculations performed on Gallium Selenide (GaSe) nano ribbons also predict that while armchair nano ribbons are all semiconductors with an indirect band gap, most of the zigzag configurations of nano ribbons were found to be metallic [20] with the possibility of showing magnetism.

This article, therefore, is an attempt to capture some of these fascinating discoveries that have laid the foundation for several new directions in materials synthesis as well as advanced application development with Group III, IV, and V Selenide based binary layered Compounds.

2.1 Indium Selenide Based Systems

InSe monolayer is a periodic hexagonal array of 4 atoms, in which Se-In-In-Se are bound by covalent bonds with some ionic character. Each atomic layer can be thought of as (111) plane of Zinc Blende structure [21]. Indium atoms share two of their valence electrons with three neighboring Se atoms. The third electron makes a covalent bond with another In atom, and the In-In bond lies perpendicular to the plane formed by Se atoms. Four out of six valence electrons of Selenium are shared with 3 In atoms (four third electrons per bond), which leaves an unbound electron lone pair on Se atom. In fact, a monolayer InSe is terminated by an electron lone pair on Se atom, which is repelled by the electron lone pair in the adjacent layers creating a van der Waals gap between layers. Few-layer InSe can come in various polytypes. In γ -InSe, Se atoms in the second layer are lined up with the first layer InSe, thus breaking the mirror symmetry available to monolayer. In the third layer, In atoms are lined up with Se atoms of the first layer.

We have evaluated the electronic band structure of mono, few-layer, and bulk γ -InSe (Fig.1). According to our results it shows drastic decrease in electronic bandgap of few layer InSe compared to that of the monolayer.

Monolayer InSe has the mirror symmetry along a direction perpendicular to the plane. Symmetry is broken when the layer number is increased. Monolayer InSe has Mexican hat like electron band structure in the valance band [22]. The valance band maximum is in the Γ-K direction, while parabolic conduction band minimum stays at the Γ point. This results in an indirect electronic bandgap in monolayer InSe. Our calculations based on ab initio density functional theory with GGA pseudopotential shows the monolayer bandgap to be 1.4 eV. Fig.1(g) shows the change in electronic bandgap as a function of the layer thickness of γ-InSe.

Other important feature is that the Mexican hat behavior diminishes as the layer number is increased. Based on photoluminescence spectroscopy, D.A. Bandurin reported a more than 0.5 eV decrease in the bilayer bandgap from bulk band gap [23]. Our calculated values are in agreement with those reported in references [23,24].

Our calculations were done using the first principles density functional theory as it is implemented in Quantum Espresso packages, with the PBE-GGA pseudopotentials. It is known that GGA does not correctly treat for the strongly correlated electrons thus underestimate the bandgap. The existing correction methods such as DFT+U or hybrid functionals only regidly shift the band gap preserving the trends of the relative changes. A set of reported values for lattice parameters and electronic bandgaps are tabulated in Table 1.

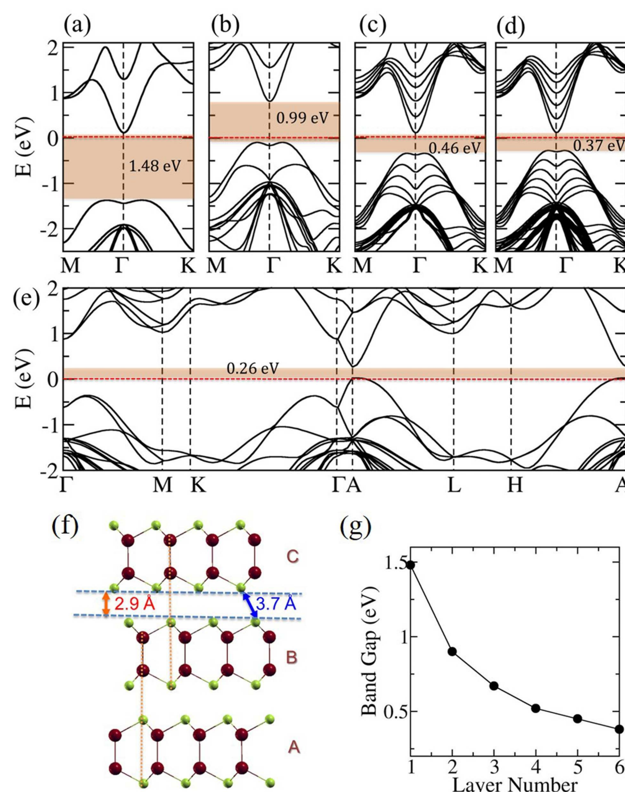

Fig. 1 Panels (a)-(d) and (e) show the electron band structure of N-layer InSe (N=1,2,5,6) and for bulk.Panel (f) shows the stacking of γ -InSe and (g) the electronic band gap Vs layer number is shown.

As evident from these aforementioned studies, one of the key difference in InSe based system is that unlike some TMD such as MoS_2, which goes to direct to indirect band transition upon increasing layer thickness, InSe shows a completely opposite behavior, i.e it goes from indirect to direct band upon increase in layer thickness. The idea of having few layer semiconductor with direct band gap in InSe systems and their polytypes such as In_2Se_3 etc. immediately opened up both theoretical as well as experimental investigations in understanding controlled growth,

View Article Online
DOI: 10.1039/C7TC02866K

Table 1 Structural parameters and electronic band gap for Group IV monochalcogenides obtained from calculations.

Material	System	Calculation method	Lattice Constant (Å) a	b	c	Bandgap (eV) Indirect	Direct	Ref.
InSe	ML	GGA	3.953	3. 953	–	1.602		25
InSe	ML	HSE06				2.16		26
InSe	ML	GW	3.99	3.99	–	2.97		24
InSe	ML	GGA	4.09	4.09	–	1.44		27
InSe	ML	GGA	4.028	4.028	–	1.61		22
InSe	Bulk	GW					1.3	24
InSe	Bulk	GGA	4.028	4.028	16.027		0.48	22
GaSe	ML	HSE06	3.77	3.77	–	3.001		28
GaSe	ML	LDA	3.65	3.65	–	3.001		28
GaSe	Bulk	LDA	3.66	3.66	15.587		1.21	29
GaSe	Bulk	GW					2.34	29
GaSe	Bulk	GGA	3.755	3.755	15.898		0.870	22
SnSe	ML	GGA	4.20	4.60	–		1.10	30
SnSe	ML	HSE06					1.69	30
SnSe	ML	GGA				0.88		31
SnSe	ML	HSE06	4.27	4.41	–	1.51		31
SnSe	ML	GGA	4.28	4.43	–	1.00		32
SnSe	ML	HSE06	4.28	4.43	–	1.44		32
SnSe	ML	GGA	4.26	4.45	–	0.93		33
SnSe	Bulk	GGA	4.45	4.16	11.5	0.5		34
SnSe	Bulk	GGA	4.47	4.22	11.81	0.55		35
SnSe	Bulk	HSE06				1.00		35
GeSe	ML	GGA	3.92	4.38	–		1.28	30
GeSe	ML	HSE06					1.68	30
GeSe	ML	GGA	4.25	3.97	–		1.11	36
GeSe	ML	GGA	3.99	4.26	–		1.15	31
GeSe	ML	HSE06					1.74	31
GeSe	ML	GGA	3.92	4.28	–	1.17		32
GeSe	ML	HSE06	3.92	4.28	–	1.71		32
GeSe	ML	GGA	3.96	4.30	–	1.14		33
GeSe	Bulk	GGA	4.41	3.84	10.89	0.866		37
GeSe	Bulk	HSE06				1.29		37

nanoscale electronics, opto-electronics properties and their associated applications [23,25–27,38–64]. Various approaches of synthesizing these materials, for example, using chemical vapor transport method [38], solution processed technique [41], physical vapor deposition [42], physical vapor transport [43] as well as utilizing Van der Waals epitaxy [64] techniques are also reported in the literature.

Initial investigations on InSe systems focused on mechanically exfoliated layers of samples grown using chemical vapor transport method [38]. Based on the results from DFT and high-field magneto optics, Mudd et al., reported a significantly smaller electron and exciton effective mass, which is weakly dependent on the layer thickness in few layer InSe. With initial evidence of few layer InSe flakes showing existence of direct band gap, apart from understanding fundamental optical properties, a vast majority of investigations focused on field effect transistors (FET) and/or photodetection abilities of these systems [40,42,43,48–52,54,56,62,64]. For example, Field-effect transistors fabricated using monolayer α -In_2Se_3 synthesized using physical vapor deposition show a p-type behavior with mobility up to 2.5 cm^2/Vs [42]. In general, several studies have shown that typical room temperature mobilities of FET fabricated using InSe flakes are few tens of cm^2/Vs. A detail list of mobility values are listed in Table 2. Techniques to enhance FET mobilities are also reported for multilayer InSe flakes [48]. In this investigation, it was found that by using a bilayer dielectric of poly-(methyl methacrylate) (PMMA)/Al_2O_3 instead of using conventional SiO_2, room temperature mobilities of 1055 cm^2/Vs can be achieved. Such back gate engineering, according to this report, can also lead to InSe based FET with a high current on/off ratios of 10^8 and strong current saturation over a broad voltage window [48]. Similarly, investigations performed on few-layer InSe encapsulated in hexagonal boron nitride under an inert atmosphere showed that carrier mobilities $> 10^3$ cm^2/Vs at room temperature [23]. This article also reported the observation of fully developed quantum Hall effect.

A large number of investigations also focused on photoconductive studies of InSe based materials. For a detail discussion of several key parameters such as responsivity (R), photoconductive gain, external quantum efficiency (EQE), response time, detectivity (D) etc., of photoconductors/photo-detector and or photo FETs the authors would refer to the article by Buscema et al. [10] which provides an excellent and in-depth study of different aspects of photocurrent generation with two-dimensional van der Waals semiconductors. Investigations performed so far indicate that above mentioned parameters of photo-detectors depend on a variety of factors such as layer thickness, growth method, device characterization parameters, wavelength and intensity of light used etc. As such reports of InSe photoconductors showing very high reponsitivities of $\sim$ 56800 A/W, $\lambda = 254$ nm [52] as well as InSe photoconductors showing reponsitivities of 0.0347 A/W, $\lambda = 532$ nm [63] can be found in the literature. Similar reports of photoresponsivity of $\sim$ 340 A/W, and response times few ms are also reported for monolayered α -In_2Se_3 synthesized using physical vapor deposition [42]. On the other hand photoresponsivity of up to $\sim 1.7 \times 10^3$ A/W at $\lambda = 633$ nm, with rise and decay

Published on 20 October 2017. Downloaded by Gazi Universitesi on 21/10/2017 19:45:29.

Journal of Materials Chemistry C Accepted Manuscript

View Article Online
DOI: 10.1039/C7TC02866K

Published on 20 October 2017. Downloaded by Gazi Universitesi on 21/10/2017 19:45:29.

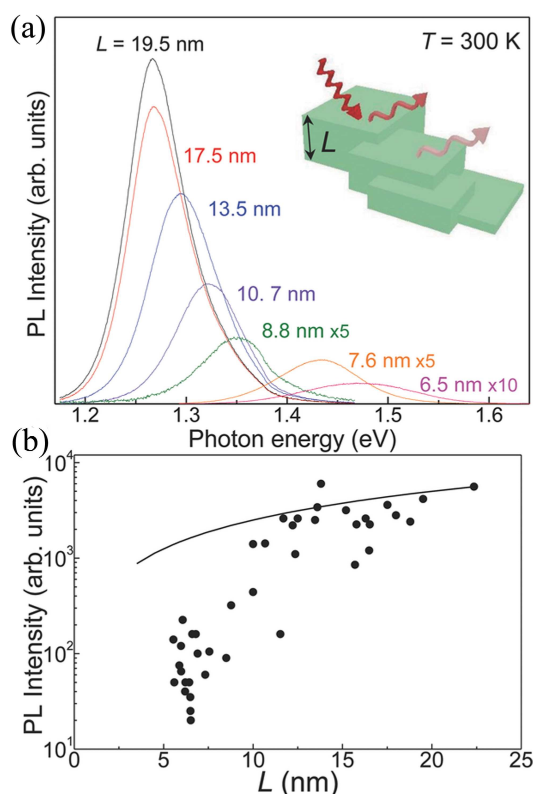

Fig. 2 (a) Typical microPL spectra of InSe layers at T = 300 K with peak energy strongly dependent on the layer thickness L (P = 0.1 mW and λ = 633 nm). The inset sketches the PL emission from flakes of different thickness L . b) L -dependence of the peak intensity of the μ PL emission. The line describes the decrease in PL intensity that would be expected from a reduction in the amount of luminescent material with decreasing L[38]. Reprinted from ref. 38, with the permission of John Wiley and Sons.

times also of the order of ~ few ms was obtained β -In_2Se_3 layers synthesizing using physical vapor transport method[43]. A recent report[54] also claims that photoresponsivity of up to ~ 10^5 A/W with $\lambda = 490$ nm, can be obtained with CVD grown In_2Se_3 layers. This study also reported a EQE % of 300000 and a detectivity ~ 10^{15} Jones[54]. A comprehensive list of figure of merit values obtained for InSe based photo detectors are listed in Table 2 along with several other materials.

There are several possible mechanisms that play an important role in determining the photo response behavior of a 2D photo-transistors. These mechanisms include photo-voltaic effect, photo-thermoelectric effect, photo-gating, etc. which can contribute to the gain mechanisms[10]. A detailed analysis of photoconduction mechanism in In_2Se_3 photo FETs was performed by Buscema et al.[62]. In case of pure photo-conduction, the photocurrent (I_{ph}) is linearly dependent on the incident photon flux. However, significant deviation from this linear relationship between the light intensity and photo-current is often time observed, as in the case of In_2Se_3 photo FETs (Fig. 3). These trapped charge carriers act as additional gating and consequently increases the carrier concentration inside the In_2Se_3 photo FETs channel.

2.2 Gallium Selenide Based Systems

Similar to InSe, Gallium Selenide also belongs to the family of Group III monochalcogenides. They both are iso-structural, 4-atom-thick layers separated by van der Waals interactions. Monolayer GaSe was synthesized by Late et al. in 2012[65]. Electronic Band gaps of mono- and bi- layer GaSe are reported to be indirect and have a value of 3.006 eV and 2.426 eV respectively, as calculated from DFT-HSE06 functional[28]. Electronic band gap decreases with increasing layer number. Bulk GaSe is reported to have a direct electronic band gap[29]. The trend of change in layer-dependent electronic band gap is similar to that of InSe.

Investigations indicate that similar to other layered systems, electronic and optoelectronic properties of GaSe devices depends upon many parameters such as growth technique, layer thickness, channel dimensions and their heterostructures[28,65–84]. In 2012, Dattaray J. Late et al. reported basic transport characteristics of micromechanically cleaved few layer GaSe sheets using back-gated FET geometry. These p-type FETs show room temperature field effect mobility of 0.6 cm^2/Vs and ~ 10^5 ON/OFF ratio[65,66]. In addition, Hai Huang et al. reported mechanically cleaved GaSe (thickness ~ 12nm) based back gated FET with room temperature field effect mobility of 0.04 cm^2/Vs and 10^2 ON/OFF ratio respectively[74]. Even though these devices showed comparatively lower mobility and ON/OFF ratio, photo responsivity of these devices reached ~ 2.2 A/W under illumination of light with wavelength of 520nm. Such finding indicate the possibility of using thin layers of GaSe as highly sensitive phototransistor[74].

The performance of GaSe based FETs, phototransistors and photodetectors can be influenced by the synthesis techniques. As example, pulsed laser deposited (PLD) GaSe nanosheet network shows photoresponsivity and EQE ranging from 0.4 A/W and 100 % at 700 nm, to 1.4 A/W and 600 % at 240 nm, respectively[72]. In this article, it was claimed that the high photoresponsivity is related to the mid-gap states of the grain boundaries in the nanosheet network. Another group of researchers recently demonstrated that the p-type GaSe nanoribbons synthesized through a one-step thermal deposition process (thickness 15nm) shows excellent spectral responsivity of 31.1 A/W and EQE of 11046 %[83].

In another recent study, layered GaSe phototransistors and photodetectors demonstrated that performance can be altered by changing the number of layers. They speculated that the increasing the carrier concentration with increasing thickness governs the resistivity of the devices and which results in the increase in photo responsivity[84]. Yufei Cao et al. systematically investigated and showed that electrode configurations can have drastic influence on the performance of these GaSe devices. In particular they showed that shrinking the spacing of the electrodes as well as using bottom contacts over top contacts can enhance the photosensitivity of few layer GaSe devices. They have shown that the photo responsivity increases from 40 to 900 A/W with electrode spacing shrinking from 10 μm to 90 nm for the top contacted devices while it increases further from 200 to 5000 A/W when bottom contacts spacing reduces from 8 μm to 290 nm[78].

Exposure to different environmental conditions can modulate

Journal of Materials Chemistry C Accepted Manuscript

View Article Online
DOI: 10.1039/C7TC02866K

Published on 20 October 2017. Downloaded by Gazi Universitesi on 21/10/2017 19:45:29.

Journal of Materials Chemistry C Accepted Manuscript

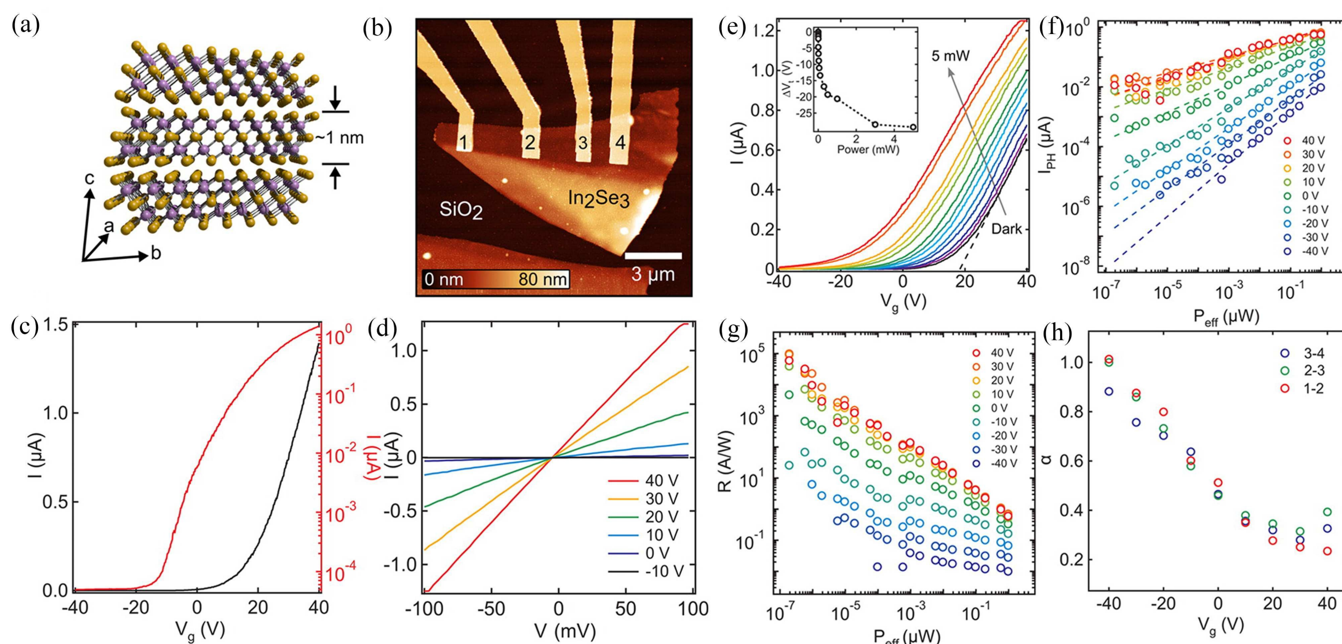

Fig. 3 (a) Crystal structure of In_2Se_3. (b) Atomic Force Microscopy scan of In_2Se_3 FET device. (c) Transfer curve for the device in b measured between contacts 3 and 4. (d) I-V curves at back-gate voltages measured between contacts 3 and 4. (e) Transfer curves with different laser illumination power (λ = 640 nm). The laser powers increase in series increments of 1, 3, 5 from 1 nW to 5 mW. Inset shows the shift of the threshold voltage for increasing powers. (f) Photocurrent versus laser power for different back-gate voltages. (g) Responsivity calculated from the measured photocurrent in panel f. (h) Exponent (α) extracted from panel f for each gate voltage[62]. Reprinted with permission from ref. 62. Copyright (2015) American Chemical Society.

the behavior of the thin GaSe devices. Shengxue Yang et al. demonstrated that mechanically exfoliated 5 nm thick GaSe can be sensitive to gas molecules. They have shown that the few-layer GaSe phototransistors exhibits improved performance under O_2 environment than air. Further, they have enhanced the photoresponse and EQE by thermal annealing the devices. Where, they claim that, chalcogen vacancies produced by thermal annealing act as active sites for the foreign molecules that increase the sensitivity to the surroundings[83].

2.3 Tin Selenide Based Systems

Group IV monochalcogenides, such as SnSe show exotic properties characterized by their structural features, layer orientation, stacking etc. which offers possible tunability to their physical properties by various structural and chemical modifications[12,34,35,85–118]

Typically, SnSe crystalizes in layered orthorhombic structure, which is a distortion form of rock salt structure[12]. There are eight atoms per unit cell forming biplaner layers along the longest axis. These layers connect through weak van der Waals interactions. Each Sn atom has seven Se neighbors. Three of them covalently bound to Sn atoms within the layers and others bound through the longer bonds. Two of the second nearest neighbours lie within the layer while the other two are in the adjacent layer as shown in Fig. 4(b).

Recent studies reported that the physical properties of SnSe are extremely sensitive to the atomistic details of its structure[87]. There is a possibility to determine the critical features of the electronic properties by modifying the atomistic structure. Based on the DFT calculation, our recent work found that the directinality of interlayer plays a major role in the details of the electronic structure. The bulk and monolayer SnSe shows the indirect band gap (Fig 4.(a)).Possible strain-induced indirect-direct transition has beed theoritically predicted[89,90].

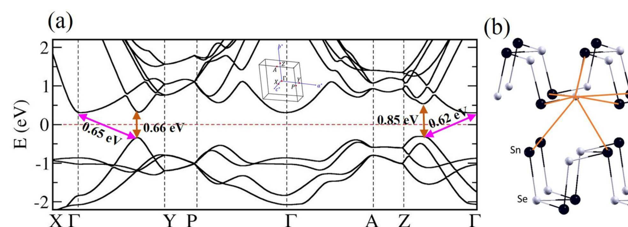

Fig. 4 (a) Electronic band structure of SnSe. The Brillouin zone for Orthorhombic structure is shown as inset (b) Atomic configuration of SnSe.

Recent investigations also indicate that apart from being classified as traditional thermoelectric materials[92–94], few layeres of SnSe systems also possess electrical/optical properties suitable for various opto-electronic applications. For example; Su et al. showed the possibility of $SnSe_2$ FET devices with high drive current capacity[97]. This study reported that the FET mobility increases from 8.6 cm^2/Vs at 300K to 28 cm^2/Vs at 77 K. Similarly Guo et al. reported high mobility FETs using few-Layer $SnSe_2$[116]. They found that it is possible to fabricate thin layer n- type $SnSe_2$ FETs with room temperature mobility 85 cm^2/Vs at 300K which

View Article Online
DOI: 10.1039/C7TC02866K

Table 2 Summary of electronic and opto-electronic properties of Selenide based materials. h-Thickness, V_D-Drain Voltage, V_G-Gate Voltage, μ-Field Effect Mobility, λ-Wavelength, P_{eff}-Effective laser power, R-Responsivity, t-Response time, D^*-Detectivity

Material	Growth Method	Dielec./ d (nm)	h (nm)	V_D (V)	V_G (V)	μ (cm^2/Vs)	I_{On}/I_{Off}	λ (nm)	P_{eff} (mW/cm^2)	R (A/W)	EQE (%)	t($x10^3$) (μs)	D^*($x10^{11}$) (Jones)	Ref.
InSe	BT[a]	SiO_2/300	12	10	70	~0.1	~ 10^4	633	2.1	157	30755	40	1	49
InSe	CVD[a]	PMMA/Al_2O_3 200/50	33	1	7	1055	~ 10^8							48
		PMMA/SiO_2 200/300	34	1	40	395								
		Al_2O_3 /50	32	1	7	64								
		SiO_2/300	33	1	40	66								
InSe	CVD[a]	SiO_2/300	32	1	40	79.5	~ 10^7							50
InSe	CVT[a]	SiO_2/285		50				543	8.8	47	344	0.06		119
InSe	CVD[a]	SiO_2/300	33	1	40	162	$10^7 - 10^8$							51
InSe	BT[a]	SiO_2/285	30	2	40	32.6	~ 10^7	254	0.29	56800		8	~ 100	52
InSe	PLD	SiO_2/300	1	1	0	10	~ 10^2	370	0.0012	27	9000	500		56
InSe	NSM[a]	SiO_2/285	5.2	3				532	250	0.0347	8.1	0.488		63
In_2Se_3	Com.[a]	SiO_2/100	3.9	5				300	0.0469	395	16300	18	23	40
In_2Se_3	PVD	SiO_2/285	~ 1	2	0	2.5	~ 10^3	532	0.026	340		6		42
In_2Se_3	PVT[a]	SiO_2	2.8 - 100	1				633		~1720	3370	2.5	~70	43
In_2Se_3	CVD[a]	SiO_2/285	~24		0	10.32	~ 10^4	490	0.29	120000	300000		~ 104	54
In_2Se_3		SiO_2/285	~ 14	0.05	30	30	~ 10^5	640		98000		9000	330	62
In_2Se_3	VWE	SiO_2/300	~ 1	0.1	0			Visible	3.27	2.5				64
GaSe	BT[a]	SiO_2/500	~ 1	0.5		0.6	~ 10^5							65
GaSe	BT[a]	SiO_2/300	4	5				254	1	2.8	1367	20		67
GaSe	VMT	SiO_2	2	10				405	50	0.017	5.2			68
GaSe	VPD	SiO_2/ 300	~ 1	-10	-60			White	1.2	8.5				70
GaSe	VWE	SiO_2/ 300	6	10				Visible	3.3	0.6				71
GaSe	PLD	SiO_2	~20	5	-30	0.1	~ 10^4	240		1.4	600			72
GaSe	Com.[a]	SiO_2/ 285	12	5	0	0.04	~ 10^2	520	0.06	2.2		30		74
GaSe	CVD[a]	SiO_2/ 300	~20-30	8		0.005		410	0.01	5000		0.27		78
GaSe	BT[a]	SiO_2/ 300	4	0.5	0	0.1		254	20	18.75	9153	210		82
GaSe	TD	SiO_2/ 300	~15	5		0.03	~ 10^2	350	3	31.1	11046		0.329	83
GaSe	Com.[a]	SiO_2/ 300	72	10				532		0.57	132.8		0.405	84
SnSe	VMT	SiO_2/ 300	15.8	0.1		1.5		White	3.5	330				104
SnSe	CVT[a]	SiO_2/ 285	~2	0.1	0	4	~ 10^3	632		0.5		2		111
SnSe	BT[a]	SiO_2/ 300	90	1		2.7	2							118
$SnSe_2$	CVD	SiO_2/ 300	21.1	1	0			800		1.9				15
$SnSe_2$	Com.[a]	SiO_2/ 110	84	2		8.6								97
$SnSe_2$	CVD	SiO_2/ 300	~1.5	3		0.6	~ 10^3	530	6.38	1100	261000	8.1	0.101	103
$SnSe_2$		SiO_2/ HfO_2 300/70	3.7			41	~ 10^4							109
$SnSe_2$	CVT[a]	SiO_2/ 300	8.6			85	~ 10^5							116
GeSe	CVD	SiO_2/ 300	60-80	4				532	6.8	2764	640000			120
GeSe	CVD[a]	SiO_2/ 300	57	4				808	283	3.5	530	~ 100		121

[a] Mechanically Exfoliated from bulk crystal, BT=Bridgeman Technique, VMT=Vapor Phase Mass Transport, VPD=Vapor Phase Deposition, VWE=Van der Waal Epitaxy, PLD=Pulsed Laser Deposition, NSM=Non-Stoicheometric Melting, Com.=Commercially available, PVD=Physical Vapor Deposition, PVT=Physical Vapor Transport, CVD=Chemical Vapor Deposition, TD=Thermal Deposition, CVT=Chemical Vapor Transport

increases to ~ 225 cm^2/Vs at 78 K. High on-off ratio up to 10^5 at 78 K were also seen in these devices. In another study, investigators evaluated a variety of combination of gating conditions on few-layer n- type $SnSe_2$ Transistors[109] and showed that it is possible to obtain $SnSe_2$ FETs with ON/OFF ratios ~ 10^4 using Hafnium Dioxide (HfO_2) back-gate as dielectric in combination with a layer of polymer electrolyte. Modulation of electrical properties of $SnSe_2$ layers using site selective doping is also reported[108]. In this article, the authors showed the possibility of achieving carrier concentration of ~ $10^{20} cm^{-3}$ by doing the $SnSe_2$ lattice using shallow electron donor such as chlorine[108]. Theoretical calculations performed by L.C Zhang et al., also predicts that it is perhaps possible to have extremely flexible monolayers of SnSe with very low lattice thermal conductivity and very high hole mobility[87].

Strong Visible-Light Absorbance in Few-Layer SnSe was reported by Shi et al.[95]. Solar cell applications using thin films of SnSe has been investigated as well[101]. Optoelectronic properties of single crystal SnSe nanoplates were evaluated by Zhao et al.[104]. They reported on controlled growth of these nanoplates on mica substrates using vapor transport deposition method. SnSe nanoplate FET devices show a p-type conduction with mobility ~ 1.5 cm^2/Vs. On white light illumination, these devices operating under 0.1 V bias between the source and drain show a current increase ~ 0.06. Typical photoresponsivity value of ~ 330 A/W was obtained. Thin layers of $SnSe_2$, grown directly on SiO_2 substrate using CVD show a photoresponsivity of 1.9 A/W, under 1 V bias between the source and drain, when illuminated with light of λ = 800 nm[15]. The possibility of utilizing $SnSe_2$ systems for high performance photo detectors are also reported by Zhou et al.[103]. In this study it was reported that few layer $SnSe_2$ can show high spectral gain ~ 1.1 x 10^3 A/W, EQE ~ 2.6 x 10^5 % and detectivity ~ 10^{10} Jones.

Chemical modification using alloying or doping to enhance the electronic properties was also observed for SnSe. Chen S et al. reported that Te doped SnSe shows the indirect band with 0.608 eV, which is smaller than the pure SnSe[91,92]. T Wei et al. reported that the band gap of Te doped SnSe keeps decreasing until the Te concentration saturates in the doped sample SnSe(1-x)Tex . This saturation value is reported as x=0.16[93]. Na doped SnSe

Published on 20 October 2017. Downloaded by Gazi Universitesi on 21/10/2017 19:45:29.

Journal of Materials Chemistry C Accepted Manuscript

View Article Online
DOI: 10.1039/C7TC02866K

Published on 20 October 2017. Downloaded by Gazi Universitesi on 21/10/2017 19:45:29.

Journal of Materials Chemistry C Accepted Manuscript

also decrease the band gap value gradually and it depends on the concentration of the doped Na [93–95].

2.4 Germanium Selenide Based Systems

Similar to tin selenide, GeSe, another member of group IV-monochalcodenides crystalizes in the distorted rocksalt structure. Several theoretical investigations are performed on this system as well [30,33,35,125–127]. Electronic band gap of GeSe is also reported to be indirect 1.14 eV (which is higher than that reported for bulk SnSe 0.86 eV. [35,125,126]. Potential applications of mono-and few layer GeSe are very similar to that of tin selenide from the same group [30,33] .

GeSe is also one of those materials whose band-gap overlaps with the solar spectrum. In the past simple chemical routes to synthesize single crystal sheets of these materials are reported [125]. These single crystals of GeSe were found to be of p-type semiconducting layered structure with a narrow band gap of 1.14 eV. Solution phase synthesis of micrometer long thin nanosheets was also reported by Xue et al. [128]. In this article, anisotropic photoresponse properties of individual micrometer-sized single-crystal GeSe nanosheets was reported. By fabricating suitable devices which probed the in plane and out of plane photoresponse properties of these nanosheets, the authors showed novel anisotropic photo switching properties. By using a white light source, the authors reported that on/off switching ratio of the device perpendicular to the layers is about 5.5, while that of the device parallel to the layers is only 1.6. Mukherjee et al. [121] reported the synthesis of high-quality, single-crystalline, micrometer-sized 2D GeSe nanosheets using vapor deposition technique. They reported that upon device fabrication with standard photo lithography process using Gold (Au) as contact electrodes, Au formed uneven Schottky barriers with GeSe nanosheet. They also demonstrated that few layer GeSe nanosheets photodetector can give rise to 3.5 A/W photo responsivity at near Infra-Red wavelength (808 nm) spectrum with EQE % $\sim$ 537. The authors claim that the formation of the SB, perhaps is one of the main contributor to the photo responsive behavior Similar, SB effects in photocurrent generation was also found in single crystalline $GeSe_2$ nanobelts grown on CVD technique. These devices showed a photo responsivity of 2764 A/W when illuminated with 532 nm light [120].

2.5 Bismuth Selenide Based Systems

Similar to other selenide-based layered materials, Bi_2Se_3, the prototypical topological insulator, shows new properties as it approaches the two-dimensional limit. A particularly intriguing finite-size effect in Bi_2Se_3 is that it transforms to an insulator at the surface, effectively behaving like conventional (trivial) insulators. Gapped surface states originate from quantum tunneling between the top and bottom surface wavefunctions in ultra-thin Bi_2Se_3. The effect was theoretically predicted to exist below 6 quintuple layers (QL) [129–131], and later also confirmed by first-principles calculations [132–134]. Experimental verification followed soon after through angle-resolved photo emission spectroscopy (ARPES) measurements [135,136]. In Fig. 5(a), we show the band structure of 2 QL Bi_2Se_3 that includes both surface and bulk bands. The well-established gamma-point surface Dirac cone of Bi_2Se_3 is gapped at the 2 QL level as evident from the 0.15 eV direct band gap. Other mechanisms such as weak localization effects also lead to surface gap opening in few-layer Bi_2Se_3, but it is of the order of meV [137,138].

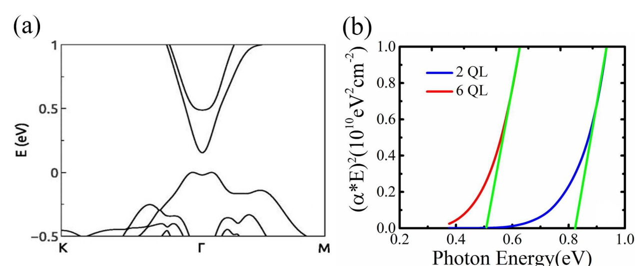

Fig. 5 (a) Band structure of 2 QL Bi_2Se_3 from first-principles calculations showing gapped surface states along with high bulk gap. Data from ref [134] . (b) Direct-gap analysis of optical spectroscopy data of 2 QL and 6 QL Bi_2Se_3 showing a blue shift in the band gap of nearly two-dimensional Bi_2Se_3 [139]. Reprinted from ref. 134 and 139, with the permission of AIP Publishing.

Another related property change originating from finite-size is the increase in the bulk band gap of few-layer Bi_2Se_3. As shown in Fig. 5(a), the lowest non-surface band lies 0.5 eV above the valence band maximum that is 0.2 eV higher than the bulk band gap of Bi_2Se_3. Very recently, optical spectroscopy measurements on our Bi_2Se_3 films grown using magnetron sputtering have validated this change in band structure [139]. In Fig. 5(b), we show the direct gap analysis data for the 2 and 6 QL Bi_2Se_3 film obtained from their optical absorption data (plot of $(\alpha\ E)^2$ vs E). The examination finds that the measured band gap of the 2 (6) QL is 0.8 (0.5) eV. The 0.3 eV blue shift is in excellent agreement with theoretical calculations [134]. An added band gap increase of nearly 0.2 eV is observed irrespective of thickness that we attribute to the Burstein-Moss effect [140]. High carrier concentration that is typical of Bi_2Se_3 leads to an apparent increase in the optical band gap. Confinement in all three directions leads to further increase in the bulk band gap to as high as 2.5 eV as demonstrated in Bi_2Se_3 nanoparticles [141]. Taken together, we find that finite-size is very effective in engineering higher band gaps in Bi_2Se_3.

The presence of gapped surface states and higher bulk band gap at the few-layer level is of significant interest for electronic applications of Bi_2Se_3. One exciting prospect is potentially higher ON/OFF ratios necessary for robust transistor performance [134]. Materials-related issues need to be addressed to achieve such potential. The presence of selenium vacancies in thin-films and single crystals generate high bulk carrier concentration ($n_{3D} > 10^{18}$ cm^{-3}) in Bi_2Se_3. As a result, the Fermi level moves to the conduction band generating n-type carriers. Few-layer Bi_2Se_3 also show high carrier concentration independent of the growth method and substrate. As the data in Table 3 indicates, both exfoliated and Physical vapor deposition grown samples (Molecular Beam Epitaxy and sputtering) show high carrier values. High values can also be induced by mechanical exfoliation [142], and exposure to ambient conditions [143,144]. Studies show that doping with Sb [145,146], electrochemical doping [142] and synthesis in Se-

View Article Online
DOI: 10.1039/C7TC02866K

Published on 20 October 2017. Downloaded by Gazi Universitesi on 21/10/2017 19:45:29.

Journal of Materials Chemistry C Accepted Manuscript

Table 3 Transport properties of few-layer Bi_2Se_3 films

Growth Method	Thickness nm	Bulk concentration ($x10^{19}$ cm^{-3})	Resistivity (300K) ($x10^{-4}$ Ω cm)	Ref.
MBE on Si(100)	3	0.028	77.4	122
	4	1.1	105	
Exfoliated on SiO_2/Si	6.5	385	1000	123
	14	107	370.3	
MBE on Al_2O_3 (0001)	2	10	12	124
	3	6.7	4.6	
	4	5	3.1	
	6	3.3	4.7	
Sputtering on amorphous quartz	6	16	15.6	This work
	4	20	20	
	3	15.6	29.5	
	2	9	370	

rich conditions[122] lower carrier concentrations in Bi_2Se_3.

Resistivity, on the hand, is strongly thickness dependent. Temperature-dependent resistivity and field-effect-transistors measurements demonstrate strong insulating behavior in 2 and 3 QL Bi_2Se_3 films[123,147,148]. As shown in Table 3, over an order of magnitude change in resistivity is recorded at room temperature on our Bi_2Se_3 films of different thicknesses grown using magnetron sputtering. A similar trend is also observed in Molecular Beam Epitaxy (MBE) grown films[124,147,148] implying, again, growth methods and conditions play a secondary role. Noteworthy is the fact that the increased resistivity of few-layer Bi_2Se_3 strongly correlates with bulk band gap increase as shown in Fig. 5. Mobilities values are low typically between 10-50 cm^2/Vs for few-layer Bi_2Se_3 [123,124,147]. Our data also indicate that enhanced scattering at the film-substrate also influences resistivity and mobility values.

3 Conclusions and Future Outlook

Although the study of atomically thin layered selenide based systems and 2D materials along with their heterostructures, have picked up its pace quite a bit in the last few years, as evident from several recent reviews[10,149–152] the field is still very new and is wide open. Some of the aspects that might play a very important role in developing these materials for a variety of advance applications are as follows. First and foremost, from the point of view of advancement in materials synthesis, efforts leading to reliable growth techniques, which will provide materials with consistent physical properties are crucial. Similarly, robust processes for large area/wafer scale synthesis of a variety of 2D layered materials systems are also needed. Techniques such as Atomic Layer Deposition (ALD), Pulse Laser Deposition (PLD), Molecular Beam Epitaxy (MBE), Sputter Deposition etc. can be explored further.

Like any other field, a tight synergy between theoretical predictions and experimental understanding of these systems will propel the field of layered selenides further.

For example, predictive modeling suggests the possible application of InSe for sensing small gas molecules[153]. Various other approaches such as oxidation[154] have been suggested for modifying the electronic properties of InSe. Similarly, strategic doping, with atomic precision of some of these selenide based compounds can lead to functionality control of these materials. For example, based on DFT calculation, X. Li et al. predicted possible n/p characteristics upon substitutional chemical doping on the anion site[155]. Similarly, many exciting possibilities exist for selenide-based topological materials, their performance in a heterostructure or hetero crystal configuration[156] and compatibility with diverse materials will be some of the factors dictating their electronic device applications.

Conflict of interest

There are no conflicts of interest to declare.

Acknowledgments

S.T. acknowledge funding support through U.S. Army Research Office MURI grant W911NF-11-1-0362.

References

1 A. H. Castro Neto, F. Guinea, N. M. R. Peres, K. S. Novoselov and A. K. Geim, *Rev. Mod. Phys.*, 2009, **81**, 109–162.

2 N. K. S. Geim, A. K., *Nature Materials*, 2007, **6**, 183–191.

3 K. S. Novoselov, Z. Jiang, Y. Zhang, S. V. Morozov, H. L. Stormer, U. Zeitler, J. C. Maan, G. S. Boebinger, P. Kim and A. K. Geim, *Science*, 2007, **315**, 1379–1379.

4 P. Miro, M. Audiffred and T. Heine, *Chem. Soc. Rev.*, 2014, **43**, 6537–6554.

5 G. R. Bhimanapati, Z. Lin, V. Meunier, Y. Jung, J. Cha, S. Das, D. Xiao, Y. Son, M. S. Strano, V. R. Cooper, L. Liang, S. G. Louie, E. Ringe, W. Zhou, S. S. Kim, R. R. Naik, B. G. Sumpter, H. Terrones, F. Xia, Y. Wang, J. Zhu, D. Akinwande, N. Alem, J. A. Schuller, R. E. Schaak, M. Terrones and J. A. Robinson, *ACS Nano*, 2015, **9**, 11509–11539.

6 G. Fiori, F. Bonaccorso, G. Iannaccone, T. Palacios, D. Neumaier, A. Seabaugh, S. K. Banerjee and L. Colombo, *Nature Nanotechnology*, 2014, **9**, 768–779.

7 H. Wang, L. Yu, Y.-H. Lee, Y. Shi, A. Hsu, M. L. Chin, L.-J. Li, M. Dubey, J. Kong and T. Palacios, *Nano Letters*, 2012, **12**, 4674–4680.

8 D.-H. Kang, J. Shim, S. K. Jang, J. Jeon, M. H. Jeon, G. Y. Yeom, W.-S. Jung, Y. H. Jang, S. Lee and J.-H. Park, *ACS Nano*, 2015, **9**, 1099–1107.

9 A. B. Kaul, *Journal of Materials Research*, 2014, **29**, 348 – 361.

10 M. Buscema, J. O. Island, D. J. Groenendijk, S. I. Blanter,

View Article Online
DOI: 10.1039/C7TC02866K

Published on 20 October 2017. Downloaded by Gazi Universitesi on 21/10/2017 19:45:29.

G. A. Steele, H. S. J. van der Zant and A. Castellanos-Gomez, *Chem. Soc. Rev.*, 2015, **44**, 3691–3718.

11 O. Lopez-Sanchez, D. Lembke, M. Kayci, A. Radenovic and A. Kis, *Nature Nanitechnology*, 2013, **8**, 497–501.

12 L.-D. Zhao, S.-H. Lo, Y. Zhang, H. Sun, G. Tan, C. Uher, C. Wolverton, V. P. Dravid and M. G. Kanatzidis, *Nature*, 2014, **508**, 373–377.

13 G. Ding, G. Gao and K. Yao, *Scientific reports*, 2015, **5**, 9567.

14 Y. Zhai, Q. Zhang, J. Jiang, T. Zhang, Y. Xiao, S. Yang and G. Xu, *Journal of Alloys and Compounds*, 2013, **553**, 270 – 272.

15 Y. Huang, K. Xu, Z. Wang, T. A. Shifa, Q. Wang, F. Wang, C. Jiang and J. He, *Nanoscale*, 2015, **7**, 17375–17380.

16 S. Lei, F. Wen, B. Li, Q. Wang, Y. Huang, Y. Gong, Y. He, P. Dong, J. Bellah, A. George, L. Ge, J. Lou, N. J. Halas, R. Vajtai and P. M. Ajayan, *Nano Letters*, 2015, **15**, 259–265.

17 A. Vargas, F. Liu and S. Kar, *Applied Physics Letters*, 2015, **106**, 243107.

18 D. Bercha, K. Rushchanskii, L. Y. Kharkhalis and M. Sznajder, **3**, 749–757.

19 P. Gopal, M. Fornari, S. Curtarolo, L. A. Agapito, L. S. I. Liyanage and M. B. Nardelli, *Phys. Rev. B*, 2015, **91**, 245202.

20 J. Zhou, *RSC Adv.*, 2015, **5**, 94679–94684.

21 P. Gomes da Costa, R. G. Dandrea, R. F. Wallis and M. Balkanski, *Phys. Rev. B*, 1993, **48**, 14135–14141.

22 D. Wickramaratne, F. Zahid and R. K. Lake, *Journal of Applied Physics*, 2015, **118**, 075101.

23 D. A. Bandurin, A. V. Tyurnina, L. Y. Geliang, A. Mishchenko, V. Zólyomi, S. V. Morozov, R. K. Kumar, R. V. Gorbachev, Z. R. Kudrynskyi, S. Pezzini *et al.*, *Nature Nanotechnology*, 2016.

24 L. Debbichi, O. Eriksson and S. Lebègue, *The journal of physical chemistry letters*, 2015, **6**, 3098–3103.

25 S. Magorrian, V. Zólyomi and V. Fal'ko, *Physical Review B*, 2016, **94**, 245431.

26 V. Zólyomi, N. Drummond and V. Fal'ko, *Physical Review B*, 2014, **89**, 205416.

27 C. Sun, H. Xiang, B. Xu, Y. Xia, J. Yin and Z. Liu, *Applied Physics Express*, 2016, **9**, 035203.

28 C. S. Jung, F. Shojaei, K. Park, J. Y. Oh, H. S. Im, D. M. Jang, J. Park and H. S. Kang, *ACS nano*, 2015, **9**, 9585–9593.

29 D. Rybkovskiy, N. Arutyunyan, A. Orekhov, I. Gromchenko, I. Vorobiev, A. Osadchy, E. Y. Salaev, T. Baykara, K. Allakhverdiev and E. Obraztsova, *Physical Review B*, 2011, **84**, 085314.

30 C. Chowdhury, S. Karmakar and A. Datta, *The Journal of Physical Chemistry C*, 2017, **121**, 7615–7624.

31 K. Cheng, Y. Guo, N. Han, Y. Su, J. Zhang and J. Zhao, *Journal of Materials Chemistry C*, 2017, **5**, 3788–3795.

32 L. Huang, F. Wu and J. Li, *The Journal of chemical physics*, 2016, **144**, 114708.

33 C. Kamal, A. Chakrabarti and M. Ezawa, *Physical Review B*, 2016, **93**, 125428.

34 Q. Wang, W. Yu, X. Fu, C. Qiao, C. Xia and Y. Jia, *Physical Chemistry Chemical Physics*, 2016, **18**, 8158–8164.

35 L. C. Gomes and A. Carvalho, *Physical Review B*, 2015, **92**, 085406.

36 I. de Oliveira and R. Longuinhos, *Physical Review B*, 2016, **94**, 035440.

37 Y. Hu, S. Zhang, S. Sun, M. Xie, B. Cai and H. Zeng, *Applied Physics Letters*, 2015, **107**, 122107.

38 G. W. Mudd, S. A. Svatek, T. Ren, A. Patanè, O. Makarovsky, L. Eaves, P. H. Beton, Z. D. Kovalyuk, G. V. Lashkarev, Z. R. Kudrynskyi *et al.*, *Advanced Materials*, 2013, **25**, 5714–5718.

39 G. Mudd, M. Molas, X. Chen, V. Zólyomi, K. Nogajewski, Z. Kudrynskyi, Z. Kovalyuk, G. Yusa, O. Makarovsky, L. Eaves *et al.*, *Scientific reports*, 2016, **6**, 39619.

40 R. B. Jacobs-Gedrim, M. Shanmugam, N. Jain, C. A. Durcan, M. T. Murphy, T. M. Murray, R. J. Matyi, R. L. Moore and B. Yu, *ACS Nano*, 2014, **8**, 514–521.

41 J. Lauth, F. E. S. Gorris, M. Samadi Khoshkhoo, T. ChassÃľ, W. Friedrich, V. Lebedeva, A. Meyer, C. Klinke, A. Kornowski, M. Scheele and H. Weller, *Chemistry of Materials*, 2016, **28**, 1728–1736.

42 J. Zhou, Q. Zeng, D. Lv, L. Sun, L. Niu, W. Fu, F. Liu, Z. Shen, C. Jin and Z. Liu, *Nano Letters*, 2015, **15**, 6400–6405.

43 N. Balakrishnan, C. R. Staddon, E. F. Smith, J. Stec, D. Gay, G. W. Mudd, O. Makarovsky, Z. R. Kudrynskyi, Z. D. Kovalyuk, L. Eaves, A. Patane and P. H. Beton, *2D Materials*, 2016, **3**, 025030.

44 S. Lei, A. Sobhani, F. Wen, A. George, Q. Wang, Y. Huang, P. Dong, B. Li, S. Najmaei, J. Bellah, G. Gupta, A. D. Mohite, L. Ge, J. Lou, N. J. Halas, R. Vajtai and P. Ajayan, *Advanced Materials*, 2014, **26**, 7666–7672.

45 J. Lauth, A. Kulkarni, F. C. M. Spoor, N. Renaud, F. C. Grozema, A. J. Houtepen, J. M. Schins, S. Kinge and L. D. A. Siebbeles, *The Journal of Physical Chemistry Letters*, 2016, **7**, 4191–4196.

46 G. W. Mudd, A. PatanÃÍ, Z. R. Kudrynskyi, M. W. Fay, O. Makarovsky, L. Eaves, Z. D. Kovalyuk, V. Zolyomi and V. Falko, *Applied Physics Letters*, 2014, **105**, 221909.

47 J. F. Sánchez-Royo, G. Muñoz-Matutano, M. Brotons-Gisbert, J. P. Martínez-Pastor, A. Segura, A. Cantarero, R. Mata, J. Canet-Ferrer, G. Tobias, E. Canadell, J. Marqués-Hueso and B. D. Gerardot, *Nano Research*, 2014, **7**, 1556–1568.

48 W. Feng, W. Zheng, W. Cao and P. Hu, *Advanced Materials*, 2014, **26**, 6587–6593.

49 S. R. Tamalampudi, Y.-Y. Lu, R. Kumar U, R. Sankar, C.-D. Liao, K. Moorthy B, C.-H. Cheng, F. C. Chou and Y.-T. Chen, *Nano letters*, 2014, **14**, 2800–2806.

50 W. Feng, W. Zheng, X. Chen, G. Liu and P. Hu, *ACS applied materials & interfaces*, 2015, **7**, 26691–26695.

51 W. Feng, X. Zhou, W. Q. Tian, W. Zheng and P. Hu, *Physical Chemistry Chemical Physics*, 2015, **17**, 3653–3658.

52 W. Feng, J.-B. Wu, X. Li, W. Zheng, X. Zhou, K. Xiao, W. Cao, B. Yang, J.-C. Idrobo, L. Basile, W. Tian, P. Tan and P. Hu, *J. Mater. Chem. C*, 2015, **3**, 7022–7028.

53 M. Brotons-Gisbert, D. Andres-Penares, J. Suh, F. Hidalgo,

Journal of Materials Chemistry C Accepted Manuscript

View Article Online
DOI: 10.1039/C7TC02866K

Published on 20 October 2017. Downloaded by Gazi Universitesi on 21/10/2017 19:45:29.

R. Abargues, P. J. Rodriguez-Canto, A. Segura, A. Cros, G. Tobias, E. Canadell, P. Ordejon, J. Wu, J. P. Martinez-Pastor and J. F. Sanchez-Royo, *Nano Letters*, 2016, **16**, 3221–3229.

54 M. Osman, Y. Huang, W. Feng, G. Liu, Y. Qiu and P. Hu, *RSC Adv.*, 2016, **6**, 70452–70459.

55 S. Deckoff-Jones, J. Zhang, C. E. Petoukhoff, M. K. Man, S. Lei, R. Vajtai, P. M. Ajayan, D. Talbayev, J. Madéo and K. M. Dani, *Scientific reports*, 2016, **6**, 22620.

56 Z. Yang, W. Jie, C.-H. Mak, S. Lin, H. Lin, X. Yang, F. Yan, S. P. Lau and J. Hao, *ACS nano*, 2017, **11**, 4225–4236.

57 M. Brotons-Gisbert, D. Andres-Penares, J. Martínez-Pastor, A. Cros and J. Sánchez-Royo, *Nanotechnology*, 2017, **28**, 115706.

58 M. A. Airo, S. Gqoba, F. Otieno, M. J. Moloto and N. Moloto, *RSC Advances*, 2016, **6**, 40777–40784.

59 C.-A. Chuang, M.-H. Lin, B.-X. Yeh, Y.-J. Chu and C.-H. Ho, *Applied Physics A*, 2017, **123**, 197.

60 X. Li, C. Xia, X. Song, J. Du and W. Xiong, *Journal of Materials Science*, 2017, **52**, 7207–7214.

61 S. Demirci, N. Avazlı, E. Durgun and S. Cahangirov, *Physical Review B*, 2017, **95**, 115409.

62 J. O. Island, S. I. Blanter, M. Buscema, H. S. van der Zant and A. Castellanos-Gomez, *Nano letters*, 2015, **15**, 7853–7858.

63 S. Lei, L. Ge, S. Najmaei, A. George, R. Kappera, J. Lou, M. Chhowalla, H. Yamaguchi, G. Gupta, R. Vajtai *et al.*, *ACS nano*, 2014, **8**, 1263–1272.

64 M. Lin, D. Wu, Y. Zhou, W. Huang, W. Jiang, W. Zheng, S. Zhao, C. Jin, Y. Guo, H. Peng *et al.*, *Journal of the American Chemical Society*, 2013, **135**, 13274–13277.

65 D. J. Late, B. Liu, H. Matte, C. Rao and V. P. Dravid, *Advanced Functional Materials*, 2012, **22**, 1894–1905.

66 D. J. Late, B. Liu, J. Luo, A. Yan, H. Matte, M. Grayson, C. Rao and V. P. Dravid, *Advanced Materials*, 2012, **24**, 3549–3554.

67 P. Hu, Z. Wen, L. Wang, P. Tan and K. Xiao, *ACS nano*, 2012, **6**, 5988–5994.

68 S. Lei, L. Ge, Z. Liu, S. Najmaei, G. Shi, G. You, J. Lou, R. Vajtai and P. M. Ajayan, *Nano letters*, 2013, **13**, 2777–2781.

69 X. Li, M.-W. Lin, A. A. Puretzky, J. C. Idrobo, C. Ma, M. Chi, M. Yoon, C. M. Rouleau, I. I. Kravchenko, D. B. Geohegan *et al.*, *Scientific reports*, 2014, **4**, 5497.

70 M. Mahjouri-Samani, M. Tian, K. Wang, A. Boulesbaa, C. M. Rouleau, A. A. Puretzky, M. A. McGuire, B. R. Srijanto, K. Xiao, G. Eres *et al.*, *ACS nano*, 2014, **8**, 11567–11575.

71 Y. Zhou, Y. Nie, Y. Liu, K. Yan, J. Hong, C. Jin, Y. Zhou, J. Yin, Z. Liu and H. Peng, *Acs Nano*, 2014, **8**, 1485–1490.

72 M. Mahjouri-Samani, R. Gresback, M. Tian, K. Wang, A. A. Puretzky, C. M. Rouleau, G. Eres, I. N. Ivanov, K. Xiao, M. A. McGuire *et al.*, *Advanced Functional Materials*, 2014, **24**, 6365–6371.

73 R. D. Rodriguez, S. Müller, E. Sheremet, D. R. Zahn, A. Villabona, S. A. Lopez-Rivera, P. Tonndorf, S. M. de Vasconcellos and R. Bratschitsch, *Journal of Vacuum Science & Technology B, Nanotechnology and Microelectronics: Materials, Processing, Measurement, and Phenomena*, 2014, **32**, 04E106.

74 H. Huang, P. Wang, Y. Gao, X. Wang, T. Lin, J. Wang, L. Liao, J. Sun, X. Meng, Z. Huang *et al.*, *Applied Physics Letters*, 2015, **107**, 143112.

75 W. Jie, X. Chen, D. Li, L. Xie, Y. Y. Hui, S. P. Lau, X. Cui and J. Hao, *Angewandte Chemie International Edition*, 2015, **54**, 1185–1189.

76 N. Seeburrun, E. F. Archibong and P. Ramasami, *Journal of molecular modeling*, 2015, **21**, 42.

77 O. Del Pozo-Zamudio, S. Schwarz, M. Sich, I. Akimov, M. Bayer, R. Schofield, E. Chekhovich, B. Robinson, N. Kay, O. Kolosov *et al.*, *2D Materials*, 2015, **2**, 035010.

78 Y. Cao, K. Cai, P. Hu, L. Zhao, T. Yan, W. Luo, X. Zhang, X. Wu, K. Wang and H. Zheng, *Scientific reports*, 2015, **5**, 8130.

79 X. Zhou, J. Cheng, Y. Zhou, T. Cao, H. Hong, Z. Liao, S. Wu, H. Peng, K. Liu and D. Yu, *Journal of the American Chemical Society*, 2015, **137**, 7994–7997.

80 J. Zhou, *RSC Advances*, 2015, **5**, 94679–94684.

81 X. Li, L. Basile, B. Huang, C. Ma, J. Lee, I. V. Vlassiouk, A. A. Puretzky, M.-W. Lin, M. Yoon, M. Chi *et al.*, *ACS nano*, 2015, **9**, 8078–8088.

82 S. Yang, Q. Yue, H. Cai, K. Wu, C. Jiang and S. Tongay, *Journal of Materials Chemistry C*, 2016, **4**, 248–253.

83 X. Xiong, Q. Zhang, X. Zhou, B. Jin, H. Li and T. Zhai, *Journal of Materials Chemistry C*, 2016, **4**, 7817–7823.

84 P. J. Ko, A. Abderrahmane, T. Takamura, N.-H. Kim and A. Sandhu, *Nanotechnology*, 2016, **27**, 325202.

85 L.-D. Zhao, C. Chang, G. Tan and M. G. Kanatzidis, *Energy & Environmental Science*, 2016, **9**, 3044–3060.

86 L.-D. Zhao, G. Tan, S. Hao, J. He, Y. Pei, H. Chi, H. Wang, S. Gong, H. Xu, V. P. Dravid *et al.*, *Science*, 2015, aad3749.

87 L.-C. Zhang, G. Qin, W.-Z. Fang, H.-J. Cui, Q.-R. Zheng, Q.-B. Yan and G. Su, *Scientific reports*, 2016, **6**, 19830.

88 S.-D. Guo and Y.-H. Wang, *Journal of Applied Physics*, 2017, **121**, 034302.

89 D. D. Cuong, S. Rhim, J.-H. Lee and S. C. Hong, *AIP Advances*, 2015, **5**, 117147.

90 M. Zhou, X. Chen, M. Li and A. Du, *Journal of Materials Chemistry C*, 2017, **5**, 1247–1254.

91 S. Chen, K. Cai and W. Zhao, *Physica B: Condensed Matter*, 2012, **407**, 4154–4159.

92 T.-R. Wei, C.-F. Wu, X. Zhang, Q. Tan, L. Sun, Y. Pan and J.-F. Li, *Physical Chemistry Chemical Physics*, 2015, **17**, 30102–30109.

93 H.-Q. Leng, M. Zhou, J. Zhao, Y.-M. Han and L.-F. Li, *Rsc Advances*, 2016, **6**, 9112–9116.

94 E. K. Chere, Q. Zhang, K. Dahal, F. Cao, J. Mao and Z. Ren, *Journal of Materials Chemistry A*, 2016, **4**, 1848–1854.

95 G. Shi and E. Kioupakis, *Nano letters*, 2015, **15**, 6926–6931.

96 D. Martínez-Escobar, M. Ramachandran, A. Sánchez-Juárez and J. S. N. Rios, *Thin Solid Films*, 2013, **535**, 390–393.

97 Y. Su, M. A. Ebrish, E. J. Olson and S. J. Koester, *Applied*

Journal of Materials Chemistry C Accepted Manuscript

View Article Online
DOI: 10.1039/C7TC02866K

Published on 20 October 2017. Downloaded by Gazi Universitesi on 21/10/2017 19:45:29.

Physics Letters, 2013, **103**, 263104.

98 L. Huang, Y. Yu, C. Li and L. Cao, *The Journal of Physical Chemistry C*, 2013, **117**, 6469–6475.

99 T. Pan, D. De, J. Manongdo, A. Guloy, V. Hadjiev, Y. Lin and H. Peng, *Applied Physics Letters*, 2013, **103**, 093108.

100 G. A. Tritsaris, B. D. Malone and E. Kaxiras, *Journal of Applied Physics*, 2013, **113**, 233507.

101 N. Makori, I. Amatalo, P. Karimi and W. Njoroge, *American Journal of Condensed Matter Physics*, 2014, **4**, 87–90.

102 F. K. Butt, M. Mirza, C. Cao, F. Idrees, M. Tahir, M. Safdar, Z. Ali, M. Tanveer and I. Aslam, *CrystEngComm*, 2014, **16**, 3470–3473.

103 X. Zhou, L. Gan, W. Tian, Q. Zhang, S. Jin, H. Li, Y. Bando, D. Golberg and T. Zhai, *Advanced Materials*, 2015, **27**, 8035–8041.

104 S. Zhao, H. Wang, Y. Zhou, L. Liao, Y. Jiang, X. Yang, G. Chen, M. Lin, Y. Wang, H. Peng *et al.*, *Nano Research*, 2015, **8**, 288–295.

105 R. Yan, S. Fathipour, Y. Han, B. Song, S. Xiao, M. Li, N. Ma, V. Protasenko, D. A. Muller, D. Jena *et al.*, *Nano letters*, 2015, **15**, 5791–5798.

106 Y. Huang, K. Xu, Z. Wang, T. A. Shifa, Q. Wang, F. Wang, C. Jiang and J. He, *Nanoscale*, 2015, **7**, 17375–17380.

107 Y. Ma, *Science Bulletin*, 2015, **20**, 1789–1790.

108 S. I. Kim, S. Hwang, S. Y. Kim, W.-J. Lee, D. W. Jung, K.-S. Moon, H. J. Park, Y.-J. Cho, Y.-H. Cho, J.-H. Kim *et al.*, *Scientific reports*, 2016, **6**, 19733.

109 T. Pei, L. Bao, G. Wang, R. Ma, H. Yang, J. Li, C. Gu, S. Pantelides, S. Du and H.-j. Gao, *Applied Physics Letters*, 2016, **108**, 053506.

110 S. Saha, A. Banik and K. Biswas, *Chemistry-A European Journal*, 2016, **22**, 15634–15638.

111 P. Yu, X. Yu, W. Lu, H. Lin, L. Sun, K. Du, F. Liu, W. Fu, Q. Zeng, Z. Shen *et al.*, *Advanced Functional Materials*, 2016, **26**, 137–145.

112 K. Tyagi, B. Gahtori, S. Bathula, N. K. Singh, S. Bishnoi, S. Auluck, A. Srivastava and A. Dhar, *RSC Advances*, 2016, **6**, 11562–11569.

113 V. Kumar, P. Kumar, S. Yadav, V. Kumar, M. Bansal and D. Dwivedi, *Journal of Materials Science: Materials in Electronics*, 2016, **27**, 4043–4049.

114 P. Perumal, R. K. Ulaganathan, R. Sankar, Y.-M. Liao, T.-M. Sun, M.-W. Chu, F. C. Chou, Y.-T. Chen, M.-H. Shih and Y.-F. Chen, *Advanced Functional Materials*, 2016, **26**, 3630–3638.

115 X. Zhou, N. Zhou, C. Li, H. Song, Q. Zhang, X. Hu, L. Gan, H. Li, J. Lü, J. Luo *et al.*, *2D Materials*, 2017, **4**, 025048.

116 C. Guo, Z. Tian, Y. Xiao, Q. Mi and J. Xue, *Applied Physics Letters*, 2016, **109**, 203104.

117 Y. Wang, L. Huang, B. Li, J. Shang, C. Xia, C. Fan, H.-X. Deng, Z. Wei and J. Li, *Journal of Materials Chemistry C*, 2017, **5**, 84–90.

118 S.-H. Cho, K. Cho, N.-W. Park, S. Park, J.-H. Koh and S.-K. Lee, *Nanoscale Research Letters*, 2017, **12**, 373.

119 S. Lei, F. Wen, L. Ge, S. Najmaei, A. George, Y. Gong, W. Gao, Z. Jin, B. Li, J. Lou *et al.*, *Nano letters*, 2015, **15**, 3048–3055.

120 B. Mukherjee, E. S. Tok and C. H. Sow, *Journal of Applied Physics*, 2013, **114**, 134302.

121 B. Mukherjee, Y. Cai, H. R. Tan, Y. P. Feng, E. S. Tok and C. H. Sow, *ACS applied materials & interfaces*, 2013, **5**, 9594–9604.

122 B. C. Park, T.-H. Kim, K. I. Sim, B. Kang, J. W. Kim, B. Cho, K.-H. Jeong, M.-H. Cho and J. H. Kim, *Nature communications*, 2015, **6**, 6552.

123 S. Cho, N. P. Butch, J. Paglione and M. S. Fuhrer, *Nano letters*, 2011, **11**, 1925–1927.

124 N. Bansal, Y. S. Kim, M. Brahlek, E. Edrey and S. Oh, *Physical review letters*, 2012, **109**, 116804.

125 D. D. Vaughn II, R. J. Patel, M. A. Hickner and R. E. Schaak, *Journal of the American Chemical Society*, 2010, **132**, 15170–15172.

126 P. Mishra, H. Lohani, A. Kundu, R. Patel, G. Solanki, K. S. Menon and B. Sekhar, *Semiconductor Science and Technology*, 2015, **30**, 075001.

127 Y. Xu, H. Zhang, H. Shao, G. Ni, H. Lu, R. Zhang, B. Peng, Y. Zhu and H. Zhu, *arXiv preprint arXiv:1704.03336*, 2017.

128 D.-J. Xue, J. Tan, J.-S. Hu, W. Hu, Y.-G. Guo and L.-J. Wan, *Advanced Materials*, 2012, **24**, 4528–4533.

129 J. Linder, T. Yokoyama and A. Sudbø, *Physical review B*, 2009, **80**, 205401.

130 C.-X. Liu, H. Zhang, B. Yan, X.-L. Qi, T. Frauenheim, X. Dai, Z. Fang and S.-C. Zhang, *Physical review B*, 2010, **81**, 041307.

131 H.-Z. Lu, W.-Y. Shan, W. Yao, Q. Niu and S.-Q. Shen, *Physical review B*, 2010, **81**, 115407.

132 W. Liu, X. Peng, X. Wei, H. Yang, G. M. Stocks and J. Zhong, *Physical Review B*, 2013, **87**, 205315.

133 J. Betancourt, S. Li, X. Dang, J. Burton, E. Tsymbal and J. Velev, *Journal of Physics: Condensed Matter*, 2016, **28**, 395501.

134 J. Sun and D. J. Singh, *Journal of Applied Physics*, 2017, **121**, 064301.

135 Y. Zhang, K. He, C.-Z. Chang, C.-L. Song, L.-L. Wang, X. Chen, J.-F. Jia, Z. Fang, X. Dai, W.-Y. Shan *et al.*, *Nature Physics*, 2010, **6**, 584–588.

136 Y. Sakamoto, T. Hirahara, H. Miyazaki, S.-i. Kimura and S. Hasegawa, *Physical Review B*, 2010, **81**, 165432.

137 Q. I. Yang, M. Dolev, L. Zhang, J. Zhao, A. D. Fried, E. Schemm, M. Liu, A. Palevski, A. F. Marshall, S. H. Risbud *et al.*, *Physical Review B*, 2013, **88**, 081407.

138 H. Wang, H. Liu, C.-Z. Chang, H. Zuo, Y. Zhao, Y. Sun, Z. Xia, K. He, X. Ma, X. Xie *et al.*, *Scientific reports*, 2014, **4**, 5817.

139 Y. R. Sapkota, A. Alkabsh, A. Walber, H. Samassekou and D. Mazumdar, *Applied Physics Letters*, 2017, **110**, 181901.

140 E. Burstein, *Physical Review*, 1954, **93**, 632.

141 A. Vargas, S. Basak, F. Liu, B. Wang, E. Panaitescu, H. Lin, R. Markiewicz, A. Bansil and S. Kar, *Acs Nano*, 2014, **8**, 1222–1230.

142 D. Kim, S. Cho, N. P. Butch, P. Syers, K. Kirshenbaum, S. Adam, J. Paglione and M. S. Fuhrer, *Nature Physics*, 2012,

Journal of Materials Chemistry C Accepted Manuscript

View Article Online
DOI: 10.1039/C7TC02866K

8, 459–463.

143 D. Kong, J. J. Cha, K. Lai, H. Peng, J. G. Analytis, S. Meister, Y. Chen, H.-J. Zhang, I. R. Fisher, Z.-X. Shen *et al.*, *ACS nano*, 2011, **5**, 4698–4703.

144 M. Brahlek, Y. S. Kim, N. Bansal, E. Edrey and S. Oh, *Applied Physics Letters*, 2011, **99**, 012109.

145 J. G. Analytis, R. D. McDonald, S. C. Riggs, J.-H. Chu, G. Boebinger and I. R. Fisher, *Nature Physics*, 2010, **6**, 960–964.

146 S. S. Hong, J. J. Cha, D. Kong and Y. Cui, *Nature communications*, 2012, **3**, 757.

147 M. Liu, C.-Z. Chang, Z. Zhang, Y. Zhang, W. Ruan, K. He, L.-l. Wang, X. Chen, J.-F. Jia, S.-C. Zhang *et al.*, *Physical review B*, 2011, **83**, 165440.

148 A. Taskin, S. Sasaki, K. Segawa and Y. Ando, *Physical review letters*, 2012, **109**, 066803.

149 C. Xie, C. Mak, X. Tao and F. Yan, *Advanced Functional Materials*, 2017, **27**, 1603886.

150 X. Zhou, Q. Zhang, L. Gan, H. Li, J. Xiong and T. Zhai, *Advanced Science*, 2016, **3**, 1600177.

151 Z. Lin, A. McCreary, N. Briggs, S. Subramanian, K. Zhang, Y. Sun, X. Li, N. J. Borys, H. Yuan, S. K. Fullerton-Shirey *et al.*, *2D Materials*, 2016, **3**, 042001.

152 F. Koppens, T. Mueller, P. Avouris, A. Ferrari, M. Vitiello and M. Polini, *Nature nanotechnology*, 2014, **9**, 780–793.

153 Y. Cai, G. Zhang and Y.-W. Zhang, *The Journal of Physical Chemistry C*, 2017, **121**, 10182–10193.

154 N. Balakrishnan, Z. R. Kudrynskyi, E. F. Smith, M. W. Fay, O. Makarovsky, Z. D. Kovalyuk, L. Eaves, P. H. Beton and A. Patanè, *2D Materials*, 2017, **4**, 025043.

155 X. Li, C. Xia, X. Song, J. Du and W. Xiong, *Journal of Materials Science*, 2017, **52**, 7207–7214.

156 A. Vargas, F. Liu, C. Lane, D. Rubin, I. Bilgin, Z. Hennighausen, M. DeCapua, A. Bansil and S. Kar, *Science Advances*, 2017, **3**, e1601741.

Published on 20 October 2017. Downloaded by Gazi Universitesi on 21/10/2017 19:45:29.

Journal of Materials Chemistry C Accepted Manuscript

View Article Online
DOI: 10.1039/C7TC02866K
Published on 20 October 2017. Downloaded by Gazi Universitesi on 21/10/2017 19:45:29.

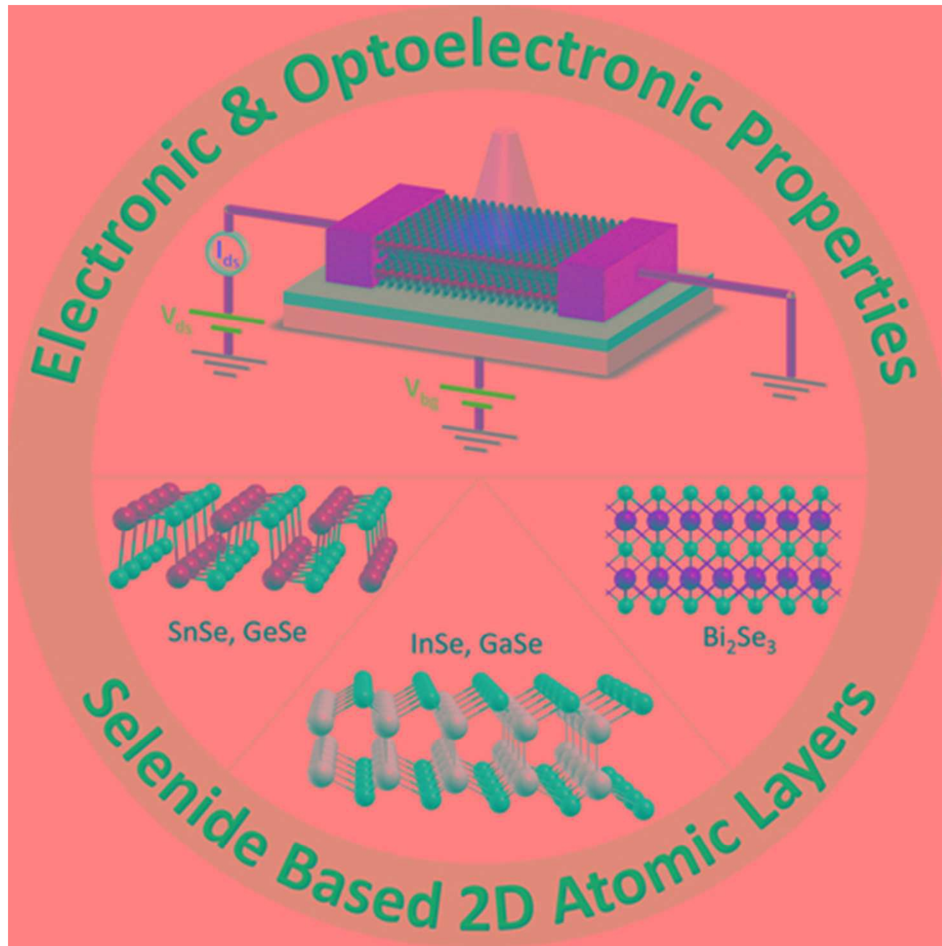

39x39mm (300 x 300 DPI)

Journal of Materials Chemistry C Accepted Manuscript